



The Journal of The Minerals, Metals & Materials Society

# **Codepositing Elements by Halide-Activated Pack Cementation**

---

Robert Bianco, Mark A. Harper, and Robert A. Rapp



# Codepositing Elements by Halide-Activated Pack Cementation

Robert Bianco, Mark A. Harper, and Robert A. Rapp

*The codeposition of two or more elements in a halide-activated cementation pack is inherently difficult because of large differences in the thermodynamic stabilities for their volatile halides. However, through a computer-assisted analysis of the pack equilibria, combinations of suitable master alloys and activator salts can be identified. The codeposition of chromium plus aluminum or chromium plus silicon by pack cementation has yielded diffusion coatings with excellent resistance to high-temperature oxidation and corrosion for a wide range of alloy substrates.*

## INTRODUCTION

In general, for oxidation resistance, a ternary alloy using the interaction of two oxidation-resistant elements is more effective than a simple binary alloy.<sup>1</sup> For example, when an alloy containing Fe-20Cr-5Al is exposed to a high-temperature oxidizing environment, initially a continuous adherent  $\text{Cr}_2\text{O}_3$  scale is formed on the surface of the alloy. This scale prevents the rapid oxidation of iron in the alloy, thereby eliminating the dissolution and inward diffusion of oxygen atoms that would otherwise cause the internal oxidation of aluminum. Escaping internal oxidation, the aluminum atoms diffuse to the  $\text{Cr}_2\text{O}_3$ /alloy interface and form an even slower-growing, more-protective  $\text{Al}_2\text{O}_3$  scale at steady state. Actually, the transient  $\text{Cr}_2\text{O}_3$  and steady-state  $\text{Al}_2\text{O}_3$  scales are quite thin, usually on the order of one to five micrometers, or a few tenths of a  $\text{mg}/\text{cm}^2$  oxygen-weight gain. Therefore, a pack-cementation process which would deposit two elements simultaneously, producing a diffusion coating with a surface containing approximately 20–30 wt.% Cr, and 4–6 wt.% Al or 2–4 wt.% Si, should be very effective in protecting low-alloy substrates from corrosive environments at high temperatures. These coatings should also provide protection from the accelerated corrosion seen when a fused-salt deposit contacts the alloy surface (hot corrosion), as occurs for certain conditions in gas turbines and fossil-fuel burning power plants. Further, alumina and silica scales are known to be more resistant than chromia in gaseous environments containing mixed oxidants (e.g., carbon plus sulfur).

Pack cementation is an in-situ chemical vapor deposition batch process that has been used to generate corrosion- and

wear-resistant coatings on inexpensive or otherwise inadequate substrates for over 75 years.<sup>2</sup> The traditional pack consists of four components: the substrate or parts to be coated, the master alloy, (i.e., a powder of the element or elements to be deposited on the surface of the parts, such as chromium and/or aluminum, chromium and/or silicon), a halide salt activator (e.g., NaCl, NaF,  $\text{NH}_4\text{Cl}$ , etc.), and a relatively inert filler powder (e.g.,  $\text{Al}_2\text{O}_3$  or  $\text{SiO}_2$ ). The master alloy, the halide salt activator, and the filler are mixed thoroughly, and the parts to be coated are buried in this mixture in a retort. The retort is heated to a high temperature (e.g., 1,000–1,150°C) while protected by an inert or reducing gas atmosphere. At the elevated temperature, the master alloy reacts with the halide activator to produce volatile metal halides that diffuse through the gas phase of the porous pack to deposit into the substrate.

An aluminizing pack-cementation process is practiced commercially for various steels and for the growth of NiAl on nickel-base superalloys for use in turbine engines.<sup>3</sup> Also, the surfaces of water wall panels in fossil-fuel power plants are enriched with chromium (chromizing). Otherwise, both processes are used

to provide coatings for chemical and petrochemical applications that must resist high-temperature corrosive environments.

The engineering of pack chemistries to deposit simultaneously two or three elements has been achieved in the past several years.<sup>4–7</sup> A variety of alloys have been coated with Cr+Al (plain-carbon and low-alloy steels, 410, 304 and 316 SS, and nickel-base alloys) and Cr+Si (plain-carbon and low-alloy steels, 304, 409 SS, and alloy 800). Because of their unique metallurgical characteristics, each alloy requires a specific pack chemistry to obtain the optimum coating composition. The ideal coating contains sufficient concentrations of the two elements for safe steady-state oxidation and corrosion resistance, without excessive contents which could lead to brittleness, unwanted phase changes, and oxidant penetration in service.

The coating elements chromium, aluminum, and silicon are ferrite stabilizers for steels. Therefore, ferritic stainless steels such as 409 SS remain ferritic at the coating temperature when Cr+Al or Cr+Si coatings are diffused into the ferritic alloy. Plain-carbon and low-alloy steels are austenitic at the coating temperature (1,000–1,050°C) and the incor-

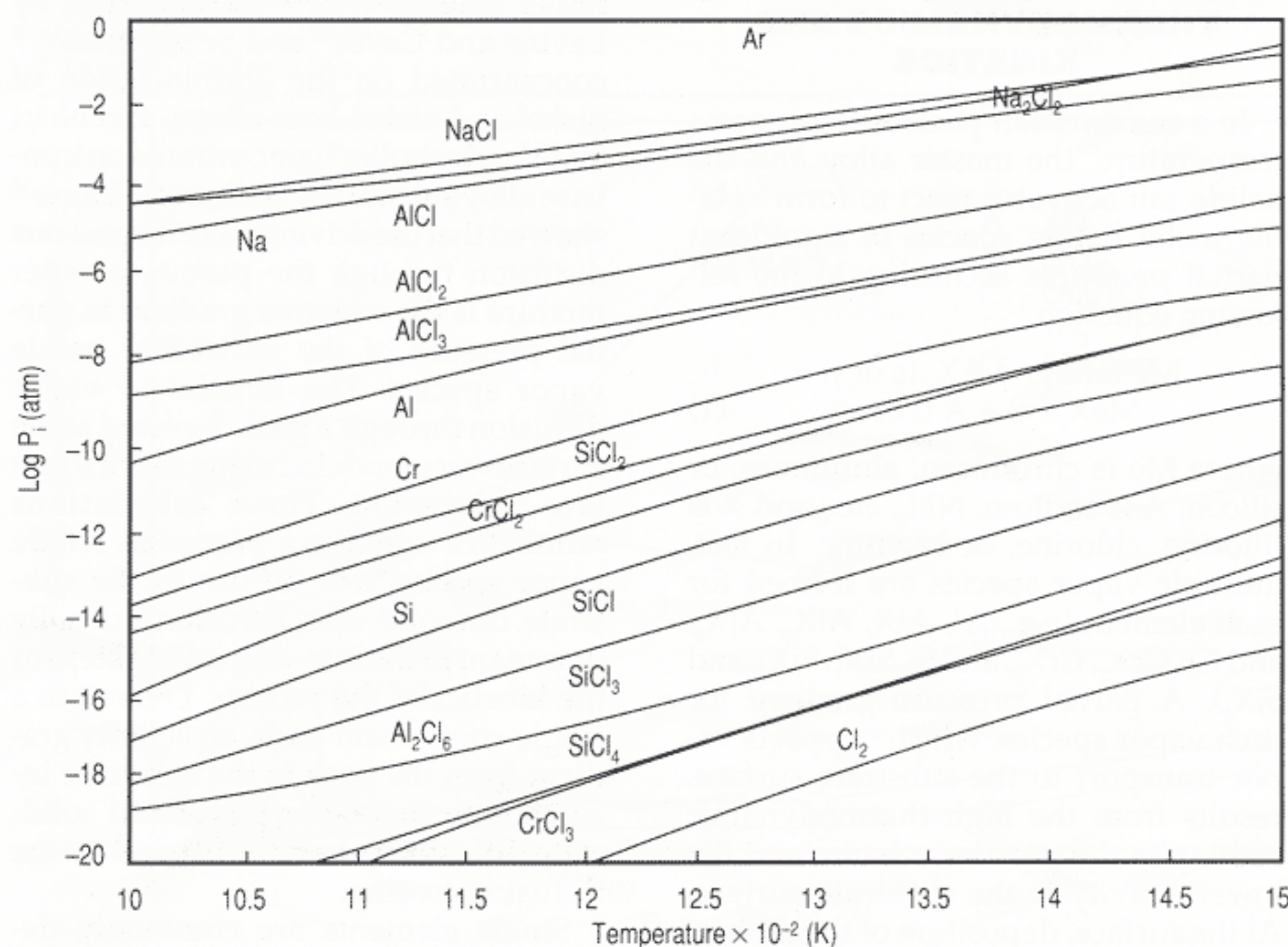


Figure 1. Log partial pressure of gaseous halides as a function of temperature in NaCl-activated packs containing pure aluminum, chromium, and silicon.



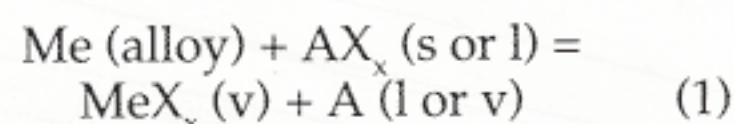
poration of Cr+Al or Cr+Si may result in the transformation of the austenite to a single-phase ferrite layer at the surface. This ferrite coating layer grows with time upon the transformation of the austenite core to a ferrite case, as dictated by the concentration gradients and the high diffusion coefficients in the ferrite.

High-alloy austenitic alloys can incorporate only limited concentrations of the coating elements into solid solution, and higher concentrations lead to a two-phase microstructure at the surface. Upon adding Cr+Al to austenitic alloys such as 304 SS and 316 SS, the inward diffusion of aluminum results in the precipitation of the compound NiAl within a ferrite matrix at the surface.<sup>5,8</sup> The resulting two-phase diffusion zone is tough mechanically and forms an alumina scale at steady state. Nickel-base superalloys, when coated with Cr+Al, form an outward-grown,  $\beta$ -NiAl plus  $\alpha$ -Cr layer, with a multiphase layer containing  $\beta$ -NiAl,  $\gamma$ -Ni<sub>3</sub>Al, and carbides present underneath. In coating with Cr+Si, the nickel silicides are generally avoided due to their low-melting eutectics, brittleness, and excessive spalling behavior upon oxidation.<sup>9</sup>

Thus, for each alloy, depending on its metallurgical factors and its intended service use, a unique pack-cementation process must be developed to produce a corrosion-resistant coating with reasonable fracture toughness and excellent adhesion to the substrate. Such Al<sub>2</sub>O<sub>3</sub>- or SiO<sub>2</sub>-forming "conversion" coatings are well bonded to the substrate by epitaxial interphase interfaces, and the coatings are inherently graded in composition so that sharp differences in physical properties such as coefficient of thermal expansion (CTE) are minimized.

## THERMODYNAMICS AND KINETICS

In a cementation pack at the process temperature, the master alloy and the halide salt activator react to form volatile metal halide species of significant partial pressures according to the following equation:<sup>10</sup>



where Me is chromium, aluminum, or silicon; A is sodium, NH<sub>4</sub>, etc.; and X is fluorine, chlorine, or bromine. In fact, multiple vapor species are formed for each element (e.g., Al, AlX, AlX<sub>2</sub>, AlX<sub>3</sub>, and Cr, CrX<sub>2</sub>, CrX<sub>3</sub>, and Si, SiX<sub>2</sub>, SiX<sub>3</sub>, and SiX<sub>4</sub>). A partial pressure gradient for each vapor species, which supports vapor transport to the substrate surface, results from the high thermodynamic activity in the powder mixture and the lower activity at the substrate surface. At the surface, deposition of the desired coating element(s) occurs via the dissociation or disproportionation of the ha-

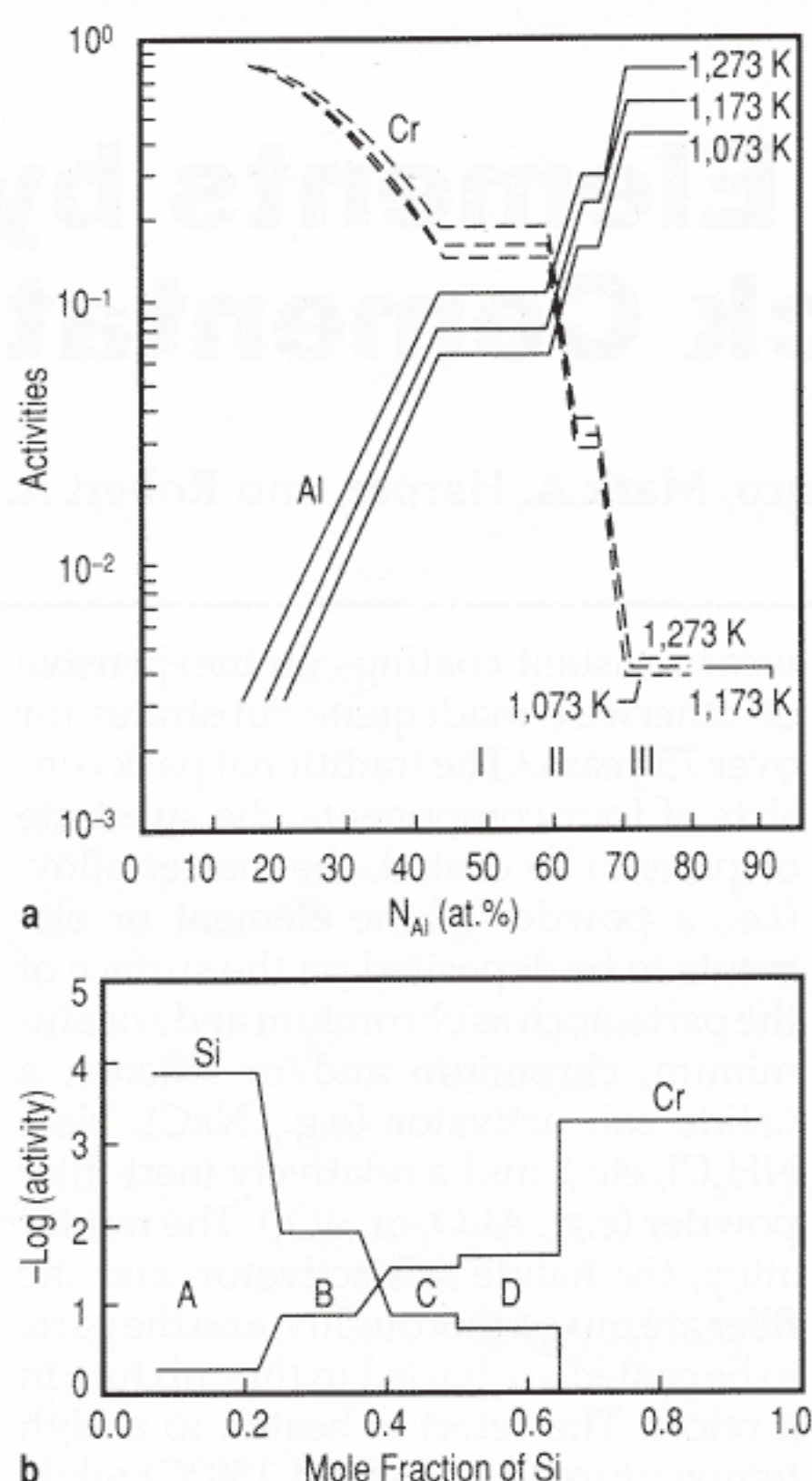


Figure 2. Activity data as a function of solute content for (a) aluminum and chromium in a Cr-Al alloy at 1,073 K, 1,173 K, and 1,273 K<sup>21</sup> and (b) silicon and chromium in a Cr-Si alloy at 1,323 K.<sup>6</sup>

lide molecules, or by a displacement reaction with the substrate.<sup>10</sup> Finally, the coating elements interdiffuse with the metallic substrate, producing some specific surface composition and microstructure or, perhaps, another phase (compound).

The thermodynamics and kinetics of pack cementation have been studied rather extensively.<sup>10-18</sup> Earlier work by Levine and Caves<sup>10</sup> and Seigle et al.<sup>11-13</sup> concentrated on the aluminization of nickel and nickel-base alloys, and Nciri and Vandenbulke<sup>15</sup> concentrated on iron-base alloy substrates. Levine and Caves<sup>10</sup> showed that the driving force for gaseous diffusion through the porous powder mixture is the negative gradient in partial pressure of the individual halide vapor species. The kinetics of vapor diffusion through a pack depleted at the surface were modeled using a Fick's first law expression. These calculations rationalize whether a particular halide vapor species will diffuse to the substrate. But solid-state diffusion is usually dominant in the rate-controlling step for the kinetics of the process. Overall in a single-component pack, an activity gradient from the pack to the substrate insures both the vapor-phase and solid-state diffusion necessary to produce the diffusion coating.

Single elements are commonly deposited into metallic substrates by the pack-cementation method, but a single-

step process which would simultaneously codeposit multiple elements (e.g., Cr-Al or Cr-Si) into metallic substrates would be more effective because the resulting coatings would exhibit superior oxidation or corrosion resistance. According to the explanation above, one might suppose that a mixture of several pure elemental powders should produce simultaneous deposition. But this prospect fails in practice. Comparable negative pressure gradients for two (or more) elements, as required for dual gaseous diffusion, essentially never occur because of large differences in the standard Gibbs energies of formation for their respective halide species (Figure 1).<sup>17,19,20</sup> However, binary chromium-rich alloys (Cr-Al and Cr-Si alloys) exhibit highly negative deviations from ideal thermodynamic behavior, so that such master alloys can be used to reduce the activities of the aluminum or silicon components by several orders of magnitude (Figures 2a and 2b).<sup>6,21</sup> Then, by using such binary alloy powders, codeposition of aluminum and chromium into nickel- or iron-base alloys, or chromium and silicon into iron-base alloys, can be achieved if an appropriately stable halide salt is also provided.<sup>4-7,22</sup> As shown in Figure 3, the dilute Cr-Al or Cr-Si master alloy powder, with reduced thermodynamic activities for aluminum or silicon, respectively, generates lower vapor pressures for these otherwise favored halide species (i.e., AlX<sub>x</sub> or SiX<sub>y</sub>).<sup>5-7,17,18</sup> In this way, the fluxes for the components to be codeposited are brought to comparable magnitudes so that simultaneous deposition results in the desired surface composition.

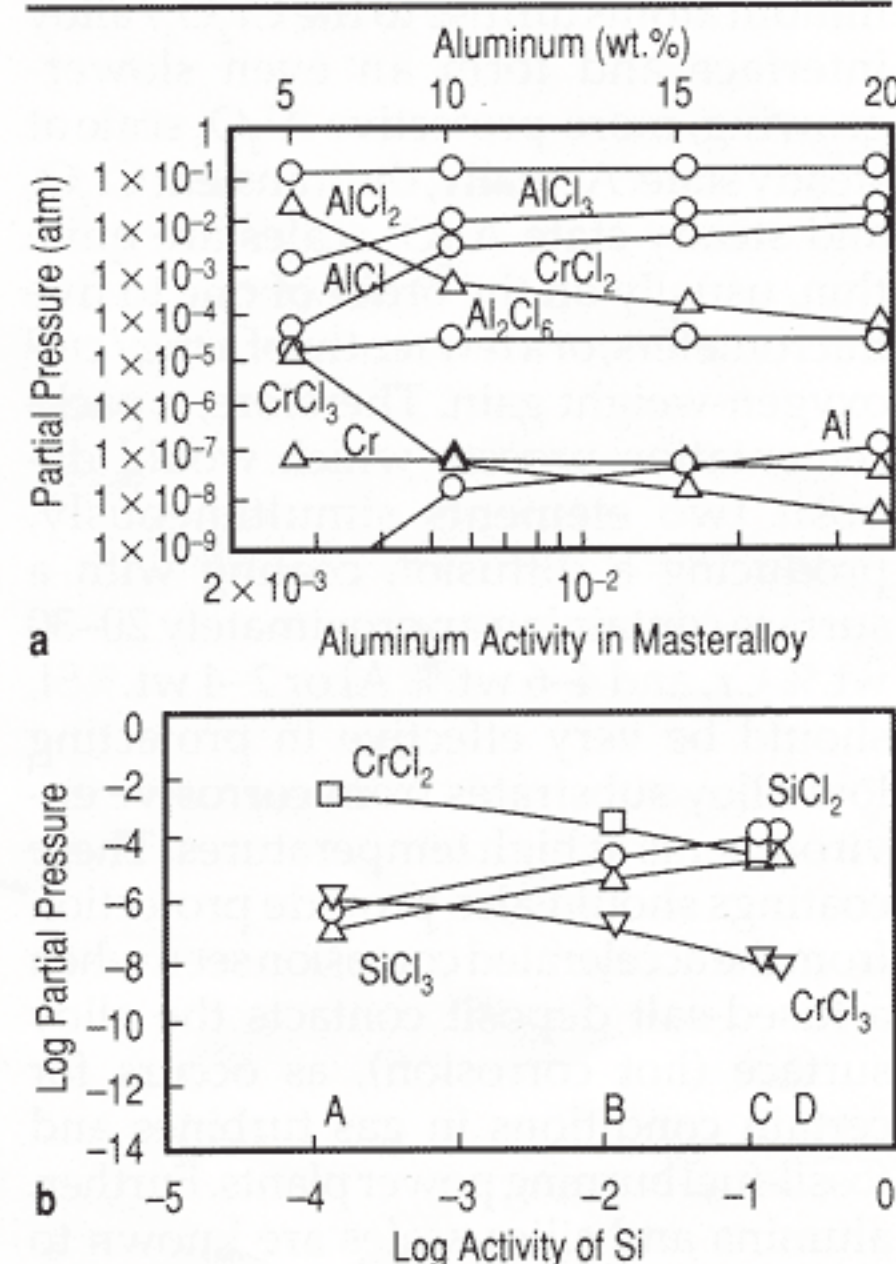


Figure 3. Equilibrium partial pressures of metallic halides in (a) NH<sub>4</sub>Cl-activated packs containing Cr-Al master alloys and Al<sub>2</sub>O<sub>3</sub> filler at 1,150°C, and (b) NaCl-activated packs containing Cr-Si master alloys and SiO<sub>2</sub> filler at 1,050°C.



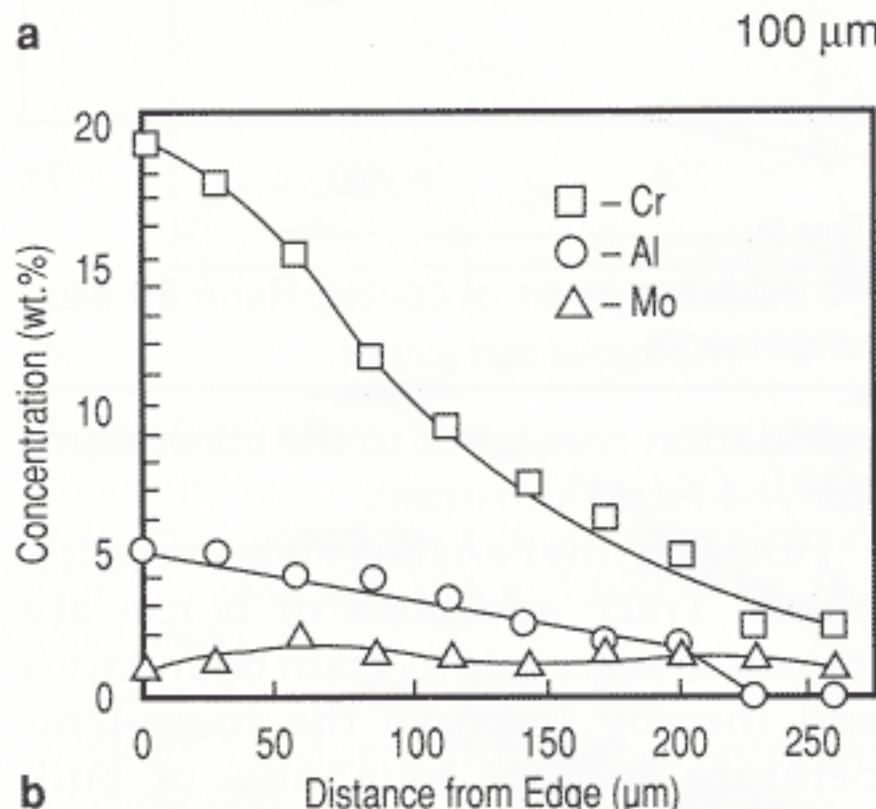
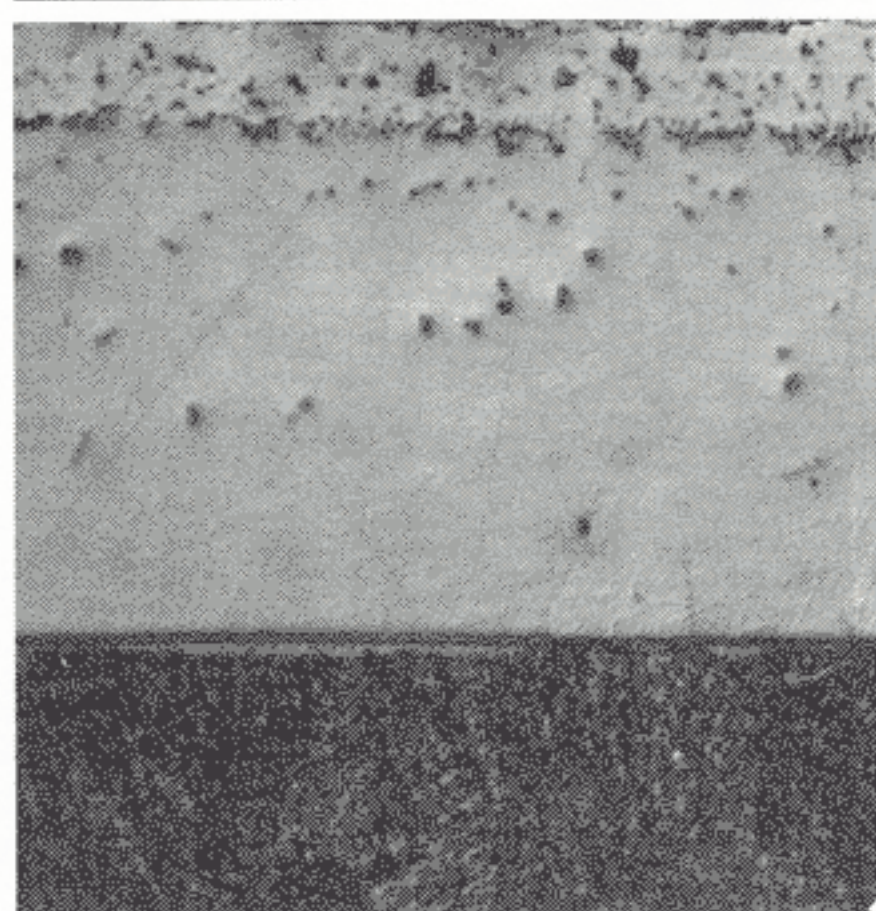


Figure 4. (a) Microstructure and (b) concentration profiles of coated Fe-2.25Cr-1.0Mo-0.15C steel using a "lean" pack of 90Cr-10Al master alloy (8 wt.% of pack) and  $\text{NH}_4\text{Cl}$  activator diffused at 1,150°C for 6 h.

In addition, a third (or fourth) minor element might also be incorporated into the coating.<sup>7</sup> Two methods have been used to produce this further doping. A small amount of an oxide source of the desired element can be added to the pack mixture, replacing some of the inert filler. In this case, the dopant oxide must be converted in the high halide activity of the pack, producing additional metal halide species according to Equation 2:



where M is zirconium, yttrium, or hafnium, and Me is aluminum or silicon. Calculations of pack equilibria using the computer program *ITSOL*<sup>23</sup> and experiments using an atmospheric pressure sampling mass spectrometer have substantiated these reduction reactions for  $\text{ZrO}_2$  and  $\text{Y}_2\text{O}_3$  additions to  $\text{Al}_2\text{O}_3$ .<sup>24</sup> By a second method, the additional element could be introduced as the halide activator source (e.g.,  $\text{ZrCl}_4$ ,  $\text{YCl}_3$ , or  $\text{HfCl}_4$ ). For example,  $\text{ZrCl}_4$  can react with a Cr-Al master alloy to produce both aluminum and chromium halides as well as significant partial pressures of the zirconium halides.<sup>7</sup> If the substrate does not contain the third element, the necessary driving force exists for some codeposition.

## CHROMIZING-ALUMINIZING

### Low-Alloy Steels

Low-alloy steels (e.g., Fe-2.25Cr-1.0Mo-0.15C) are commonly used in utility boilers, petrochemical plants, and coal gasification systems because of their excellent creep strength in service. These materials are exposed to a variety of corrosive environments, thereby requiring surface modification to improve the corrosion resistance of the substrate. A single-step, pack-cementation process has been developed to produce the Kanthal composition (Fe-20Cr-4.5Al) on the surface of Fe-2.25Cr-1.0Mo-0.15C alloys. Figure 4 shows a micrograph and concentration profile of the alloy coated in a pack containing 8 wt.% of a 90Cr-10Al master alloy,  $\text{NH}_4\text{Cl}$  activator, and  $\text{Al}_2\text{O}_3$  filler heated at 1,150°C for 6 h. A ferrite layer is formed initially on the substrate surface, allowing for subsequent diffusion of chromium and aluminum into the ferrite matrix. Because ferrite has a very low carbon solubility, the rejection of carbon into the austenite phase at the ferrite/austenite interface prevents the formation of an  $\text{M}_{23}\text{C}_6$  carbide at the surface. The resulting Cr/Al-enriched surface provides excellent steady-state oxidation resistance by an

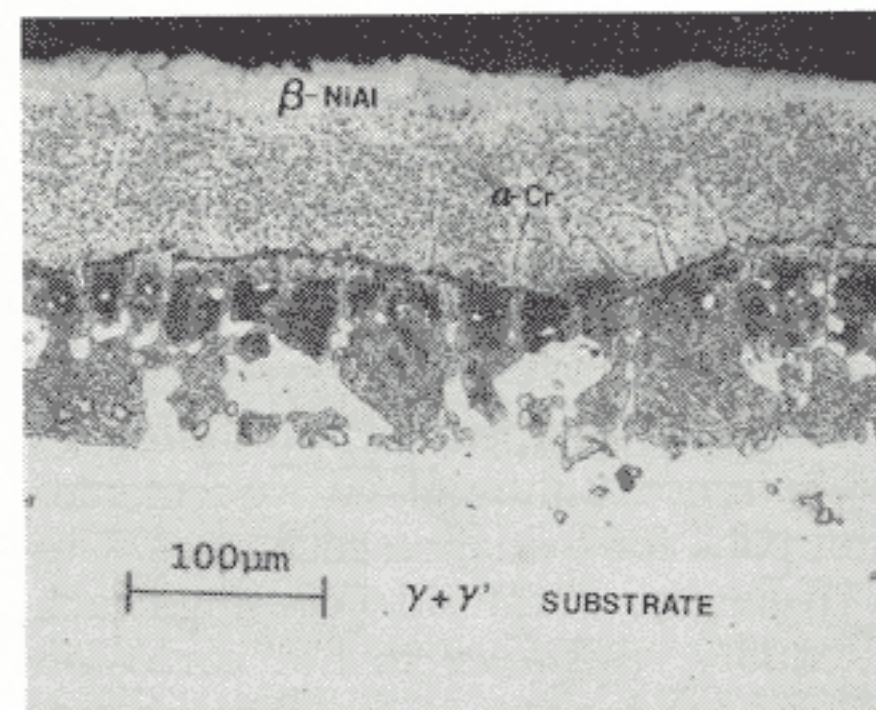


Figure 5. A cross-sectional micrograph of a René 80 alloy substrate treated at 1,150°C for 24 h in a 2 wt.%  $\text{ZrO}_2$  and  $\text{NH}_4\text{Cl}$ -activated pack (above-pack) with 25 wt.% of a 90Cr-10Al master alloy.

$\text{Al}_2\text{O}_3$  scale, even at temperatures as low as 700°C.

### Stainless Steels

Chromized-aluminized coatings were achieved on several austenitic steels (e.g., 304 SS, 316 SS, and alloy 800).<sup>5</sup> Sufficient amounts of chromium and aluminum to produce alumina-forming coatings were incorporated into each alloy. The coating morphologies consisted of particles of  $\beta\text{-NiAl}$  in a ferrite matrix, thus producing a mechanically tough microstructure. Compared to the initial work

Table I. Surface Analysis Results (EPMA) of René 80 Substrates Coated for 24 Hours at 1,150°C in Argon Gas

Activator	Master Alloy	Avg. Bulk Surface Composition (at.%)				
		Ni	Al	Cr	Zr	Y
$\text{NH}_4\text{Cl}$ , $\text{ZrO}_2$ *	92.5Cr-7.5Al (25 wt.%)	47.6	36.2	7.6	0.18	—
$\text{ZrCl}_4$ , 4 wt.%	92.5Cr-7.5Al (25 wt.%)	49.9	33.4	8.1	0.22	—
$\text{NH}_4\text{Cl}$ , $\text{Y}_2\text{O}_3$ †	92.5Cr-7.5Al (25 wt.%)	47.9	38.9	6.4	—	0.02
$\text{YCl}_3$ , $\text{Y}_2\text{O}_3$ ‡	92.5Cr-7.5Al (25 wt.%)	50.2	36.7	6.3	—	0.01
$\text{YCl}_3$ , $\text{CrCl}_2$ (1:1)	92.5Cr-7.5Al (25 wt.%)	47.7	37.2	7.6	—	0.02
$\text{YCl}_3$ , $\text{CrCl}_2$ (2:1)	92.5Cr-7.5Al (20 wt.%)	50.9	34.8	7.5	—	0.00
$\text{ZrCl}_4$ , 4 wt.%	90Fe-10Al (25 wt.%)	44.5	40.9	1.9	0.12	—

\* 2 wt.%  $\text{ZrO}_2$

† 4 wt.%  $\text{Y}_2\text{O}_3$

‡ 4 wt.%  $\text{YCl}_3$  and 4 wt.%  $\text{Y}_2\text{O}_3$

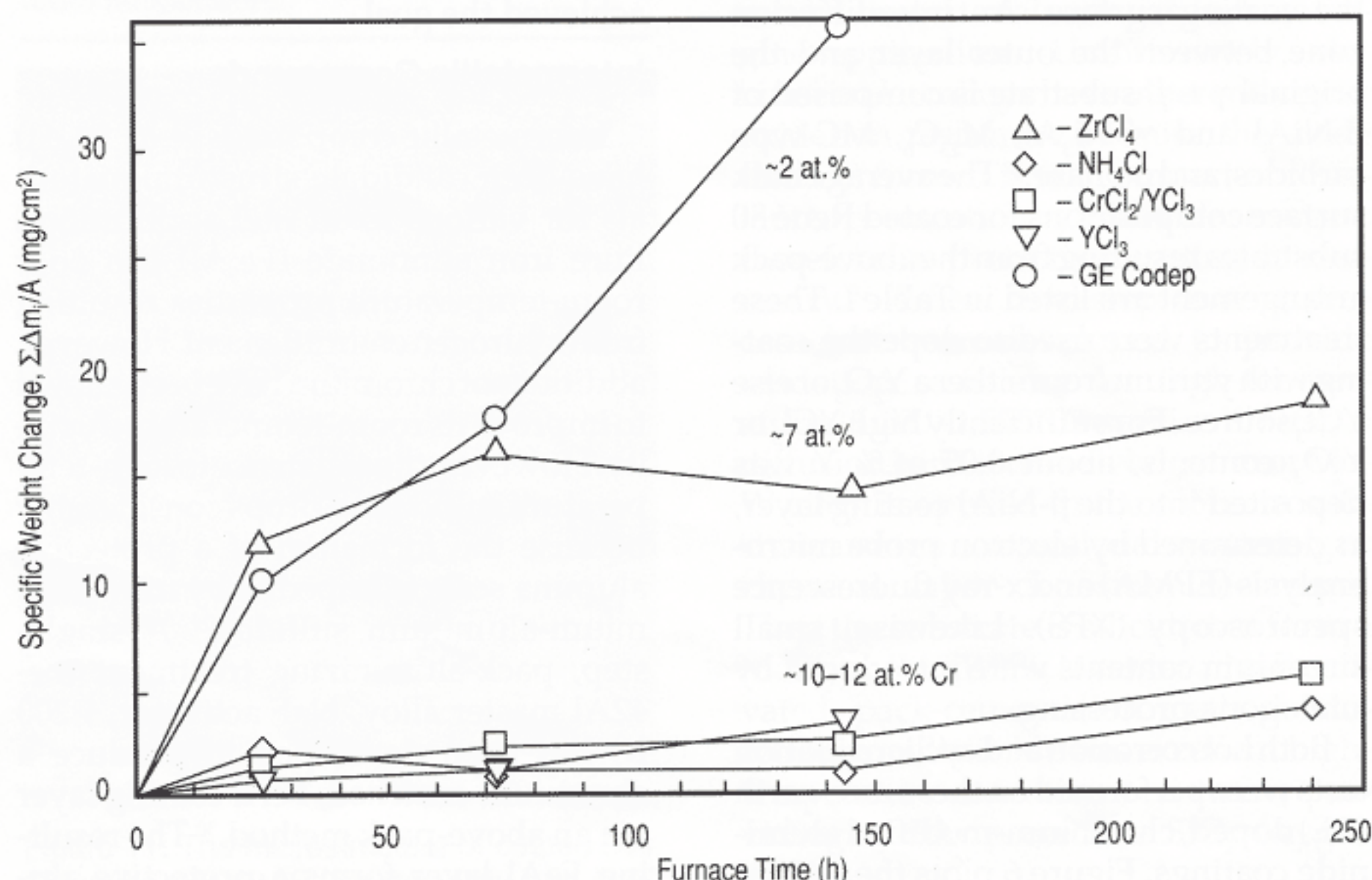


Figure 6. Isothermal hot corrosion of a René 80 alloy substrate coated by a powder-contacting method in 0.1%  $\text{SO}_2/\text{O}_2$  at 900°C with periodic  $\text{Na}_2\text{SO}_4$  recoating.



by Bangaru and Krutenat,<sup>8</sup> the use of a Cr-Al master alloy reduces the tendency for formation of an outward grown external NiAl layer that is brittle and entraps pack particles.

### Nickel-Base Superalloys

Nickel-base superalloy turbine blades are commonly aluminized in a cementation pack for oxidation resistance. Unfortunately, aluminide coatings lack adequate resistance to hot corrosion caused by deposits of fused alkali sulfates. A chromium-modified aluminide coating would promise substantial improvements in the hot corrosion resistance of the coating.<sup>25</sup> In addition, a small amount of a reactive element (zirconium or yttrium) is known to improve the adherence of the protective alumina scales.<sup>26,27</sup>

Two pack arrangements were used in the laboratory to produce chromium-enriched, aluminide coatings on several superalloys. By the simpler "powder contact" arrangement, the substrate is buried in direct physical contact with the powder mixture. By this method, some inert filler ( $\text{Al}_2\text{O}_3$ ) and master alloy particles are entrapped within the outer layer of the coated substrate. Such entrapped pack powder can act as an initiation site for thermal fatigue cracks or for local hot-corrosion attack.<sup>7</sup> Such pack entrapment, however, can be eliminated by an "above-pack" arrangement, whereby the test coupon is held isolated from contact with the pack by porous alumina cloth.

Figure 5 shows the microstructure of an  $\text{Al}_2\text{O}_3$ -free, chromium-alloyed  $\beta$ -NiAl coating, with zirconium dopant also deposited from the gas phase.<sup>7</sup> In this outward-grown  $\beta$ -NiAl coating, a dispersion of  $\alpha$ -Cr particles are precipitated near the original substrate surface and also grow inward from the gas phase at the coating surface. An interdiffusion zone between the outer layer and the original  $\gamma + \gamma'$  substrate is comprised of  $\beta$ -NiAl and  $\gamma'$ -Ni<sub>3</sub>Al,  $\text{M}_{23}\text{C}_6$ , MC-type carbides, and  $\sigma$  phase.<sup>28</sup> The average bulk surface compositions for coated René 80 substrates resulting from the above-pack arrangement are listed in Table I. These treatments were used to dope the coating with yttrium from either a  $\text{Y}_2\text{O}_3$  or else  $\text{YCl}_3$  source. For sufficiently high  $\text{YCl}_3$  or  $\text{Y}_2\text{O}_3$  contents, about 0.05 at.% Y was deposited into the  $\beta$ -NiAl coating layer, as determined by electron probe microanalysis (EPMA) and x-ray fluorescence spectroscopy (XFS). Likewise, small zirconium contents were introduced by analogous processing.

Both hot corrosion and cyclic oxidation tests were performed on these rare-earth (RE) doped, chromium-modified aluminide coatings. Figure 6 plots the weight changes for isothermal hot corrosion tests conducted for various exposure times

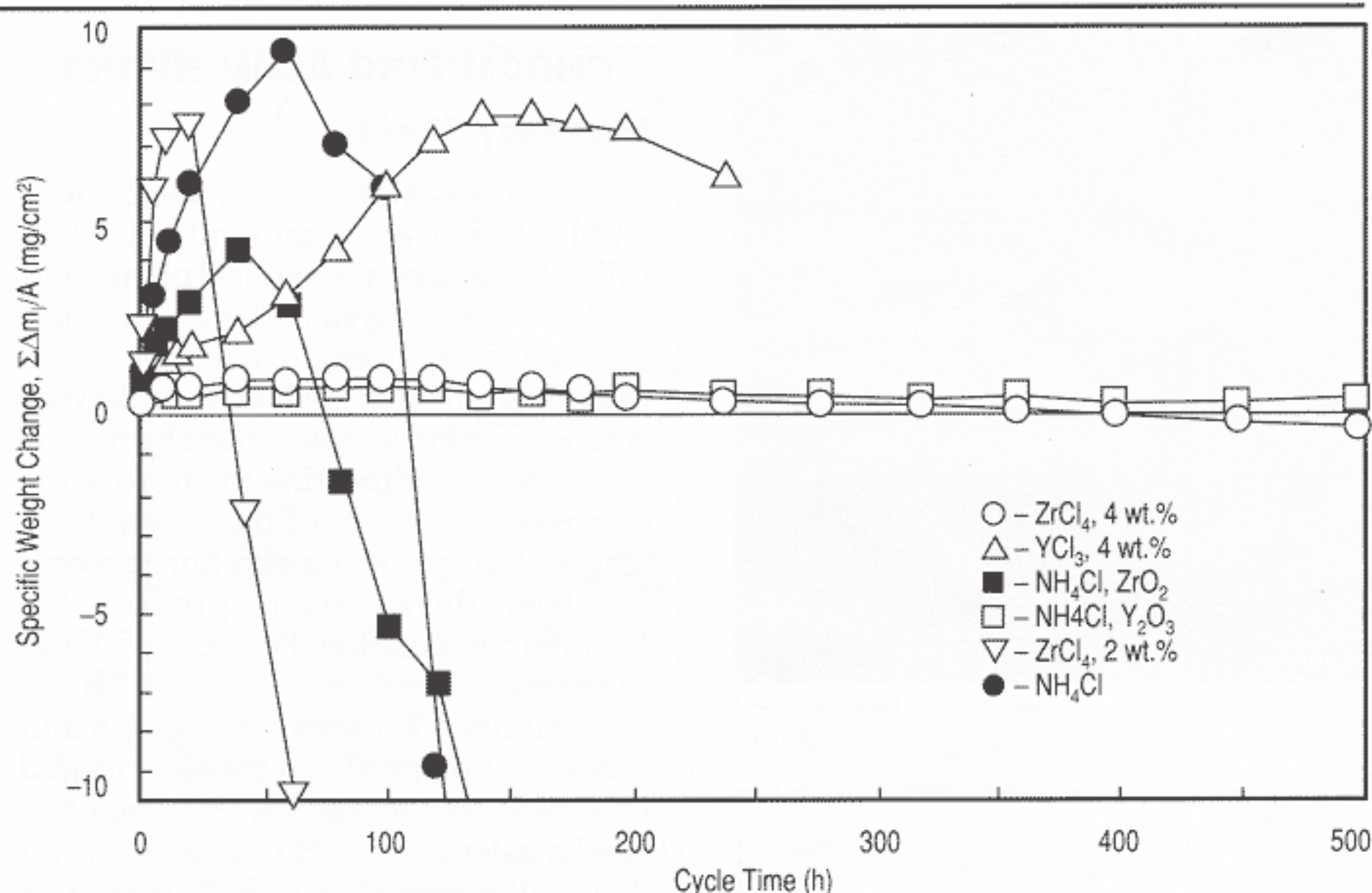


Figure 7. Specific weight changes for 1,100°C cyclic oxidation in air of coated René 80 alloy substrates versus cycle time for the above-pack arrangements.

using a 5 mg/cm<sup>2</sup> film of  $\text{Na}_2\text{SO}_4$  applied prior to each exposure period. A commercial low-activity aluminide coating, GE Codep, and the lower-chromium,  $\text{ZrCl}_4$ -activated coatings did not adequately protect the nickel-base superalloy during hot-corrosion simulation, but the higher-chromium aluminide coatings provided a substantial improvement in coating lifetime.<sup>7,25</sup>

Figure 7 is a plot of the weight changes for cyclic oxidation tests at 1,100°C of coatings prepared by the above-pack arrangements. Two of the Cr/RE-modified coatings produced acceptable protective scales of  $\alpha$ - $\text{Al}_2\text{O}_3$  and  $\text{NiAl}_2\text{O}_4$  spinel for 500 one-hour cycles. Coating failures occurred for RE-free and RE-lean coatings. As an important conclusion of this work, while every attempt to introduce both chromium and the RE into NiAl was not successful, indeed certain conditions were identified which achieved the goal.

### Intermetallic Compounds

Intermetallic compounds (e.g.,  $\text{Fe}_3\text{Al}$ ) have been candidate structural materials for various fossil fuel applications. Pure iron aluminide ( $\text{Fe}_3\text{Al}$ ) has poor room-temperature properties resulting from hydrogen embrittlement. However, additions of chromium have been shown to improve its room-temperature ductility. However, the resistance to high-temperature sulfidation drops considerably because the formation of a protective alumina scale is impeded by iron-chromium-aluminum sulfides.<sup>29</sup> A single-step, pack-aluminizing treatment (Fe-42Al master alloy, NaF activator, 1,200 K) has been developed to produce a chromium-enriched, FeAl coating layer via an above-pack method.<sup>30</sup> The resulting FeAl layer forms a protective alumina scale during oxidation exposure and provides excellent oxidation and

sulfidation resistance to the chromium-alloyed  $\text{Fe}_3\text{Al}$  substrate.

However, the FeAl layer is also a brittle phase. Trace additions of boron are known to segregate to grain boundaries and thereby improve the room-temperature fracture toughness of bulk FeAl.<sup>31</sup> An FeAl coating layer with small additions of boron (1–3 at.%) was produced by codeposition of aluminum and boron in a pack containing 0.5–1 wt.% FeB.<sup>30</sup> The boron addition reduced the microhardness of the FeAl layer from a

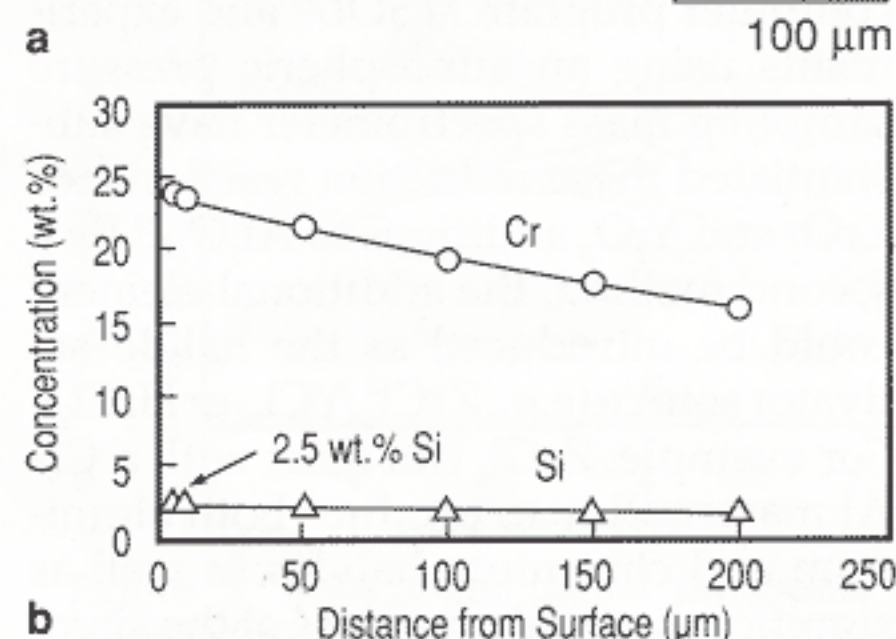


Figure 8. (a) Microstructure of coating and (b) concentration profiles for 409 SS using 90Cr-10Si master alloy and NaF activator diffused at 1,050°C for 16 h ( $\text{SiO}_2$  filler).



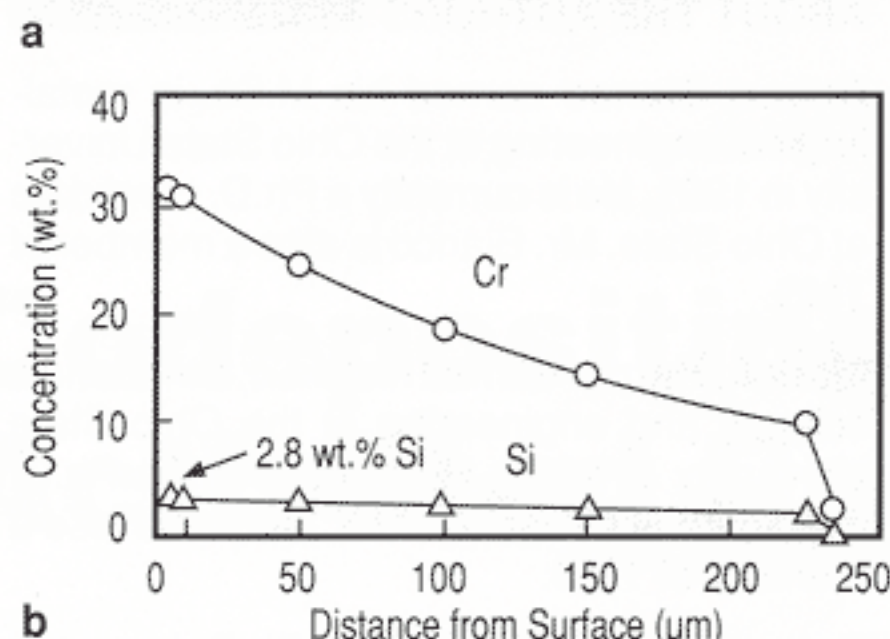
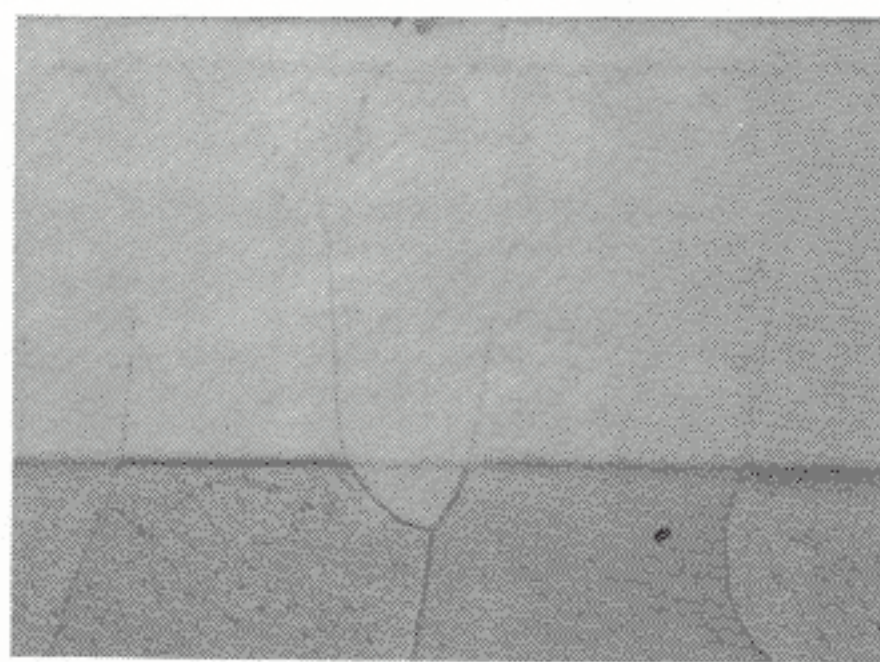


Figure 9. (a) Microstructure of coating and (b) concentration profiles for Fe-0.5Cr-0.5Mo-0.1C steel using a 90Cr-10Si master alloy and NaF activator diffused at 1,050°C for 16 h (SiO<sub>2</sub> filler).

Vickers hardness number of approximately 500 to 350. As for bulk boron-doped FeAl,<sup>32</sup> the presence of boron in the FeAl coating increased scale spallation during cyclic oxidation in air at 900°C. However, the weight losses were still below 2.5 mg/cm<sup>2</sup> after 1,000 h.<sup>30</sup>

## CHROMIZING-SILICONIZING

### Ferritic Stainless Steel

In Figure 8, the microstructure and concentration profiles for a chromized/siliconized coating on a ferritic 409 SS alloy are shown. The thin, dark horizontal line in the micrograph is the original coupon surface, showing some minor contribution by outward diffusion to coating growth. No substrate/coating interface is introduced in the absence of any phase change during the coating process, and the dominant inward diffusion excludes both porosity and pack entrapment. The surface composition is Fe-23Cr-2.5Si. Although no corrosion testing has yet been performed for the coating, this composition should provide excellent resistance to corrosion in aqueous environments and in high-temperature gaseous environments.

### Low-Alloy Steels

Figure 9 illustrates the microstructure and concentration profiles for a chromized/siliconized Fe-0.5Cr-0.5Mo-0.1C steel. Similar results were obtained for an AISI 1018 steel and an Fe-2.25Cr-1.0Mo-0.15C alloy.<sup>33</sup> Again, the surface composition is high in chromium (25 wt.% Cr) with approximately 3 wt.% Si. As shown in Figure 10, this coating has been tested in cyclic oxidation in air at

700°C and has shown extremely slow oxidation kinetics with no detectable spalling of the oxide scale. The remarkably low weight gain (less than 0.2 mg/cm<sup>2</sup> for over 4.4 months at 700°C) for the coated Fe-2.25Cr-1.0Mo-0.15C alloy has also been found for a similarly coated AISI 1018 steel. The very slow kinetics result from a slow-growing silica layer beneath a thin outer chromia scale. Also shown for comparison in Figure 10 are the isothermal oxidation kinetics of an uncoated Fe-2.25Cr-1.0Mo-0.15C alloy<sup>34</sup> and an Fe-25Cr binary alloy.<sup>35</sup> This Cr-Si coating has also shown negligible corrosion in an aerated 3.5% NaCl aqueous solution at room temperature.

### Austenitic Steels

As mentioned above, austenitic alloys can be coated by diffusing the coating elements into solid solution or by transforming the matrix into a ferrite-plus-austenite two-phase field. For example, about 3 wt.% Si was diffused into the surface of the austenitic alloy 800 without a significant change in microstructure. In contrast, Figure 11 shows the transformation at the surface for 304 SS upon chromizing/siliconizing to form

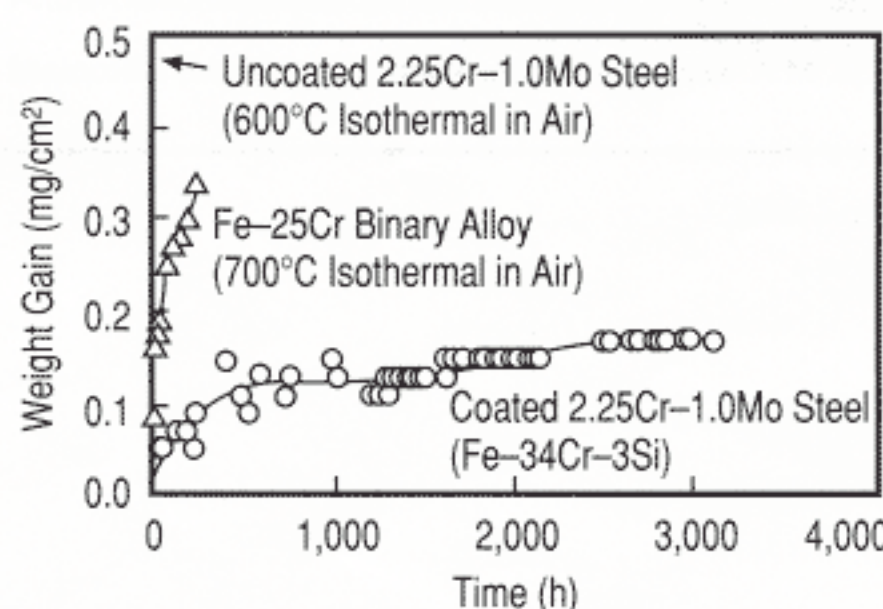


Figure 10. A plot of weight gain vs. time for the cyclic oxidation in air at 700°C of coated samples with surface compositions of 34Cr-3Si. Each indicated point represents the weight gain measured after cooling from 700°C to room temperature.

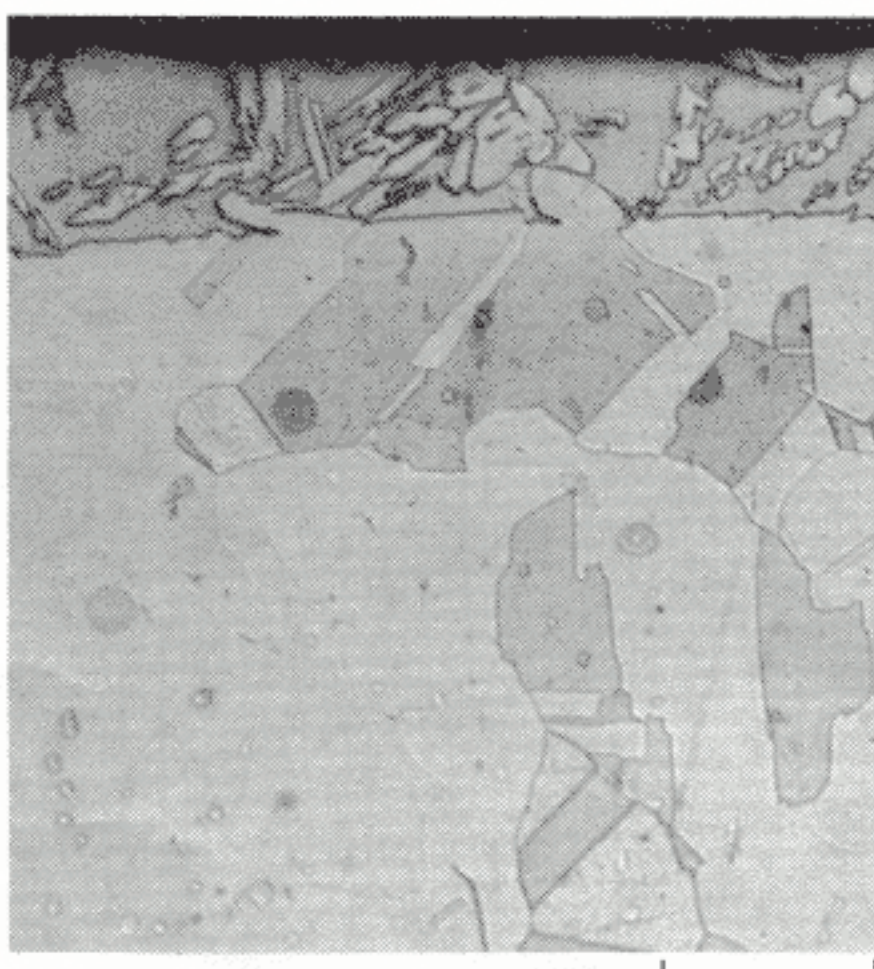


Figure 11. The microstructure of coated 304 SS using 90Cr-10Si master alloy and NaF activator diffused at 1,150°C for 16 h (Al<sub>2</sub>O<sub>3</sub> filler).

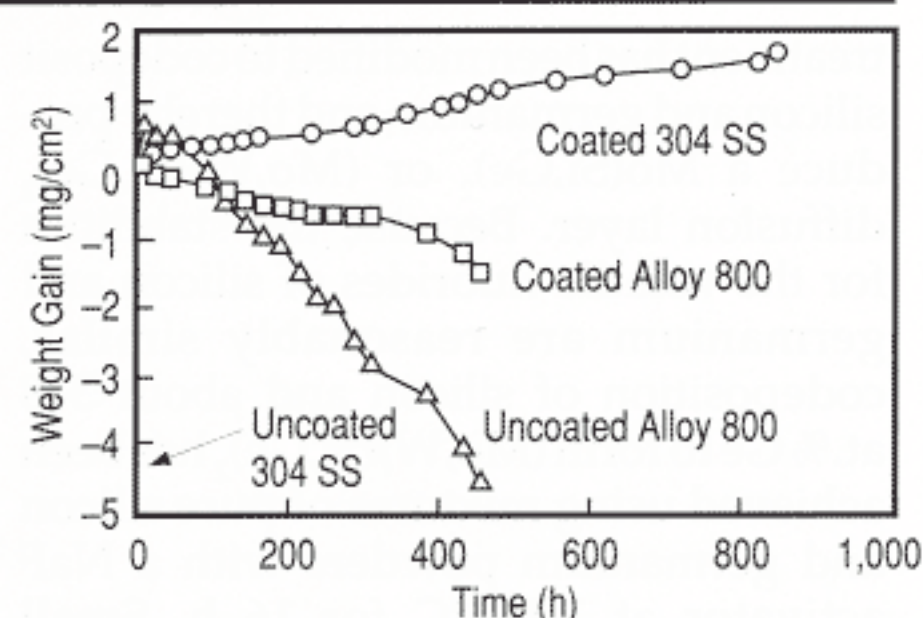


Figure 12. A plot of weight gain vs. time for the cyclic oxidation in air at 1,035°C of coated and uncoated 304 SS and alloy 800. Each indicated point represents the weight gain measured after cooling from 1,035°C to room temperature.

ferrite plus austenite.<sup>36</sup> Figure 12 presents the oxidation kinetics for these two coated alloys compared to the uncoated alloys upon cyclic oxidation at 1,035°C in air. The coated alloy 800 does suffer some scale spallation upon temperature cycling (approximately one percent of the surface area), but this behavior is an important improvement over the uncoated alloy. The coated 304 SS exhibited excellent high-temperature oxidation resistance with no evidence of spalling, whereas the uncoated alloy did not form an effective adherent protective scale.

A key element in the reduction of oxidation kinetics is the presence of ferrite, with its much higher diffusion coefficients, at the surface. The high diffusivity for ferrite promotes the early formation and retention of the thermodynamically more stable oxide scales (i.e., chromium oxide rather than iron oxide at an early stage of oxidation, and silica rather than chromia at steady state).

### Niobium-Base Alloys

Because of their high solidus temperatures and reasonable creep strengths, niobium alloys have been considered as candidate materials for gas turbine engine applications. Unfortunately, niobium and its alloys have inherently poor oxidation resistance because the oxide (Nb<sub>2</sub>O<sub>5</sub>) formed is not compact or resistant to permeation by molecular oxygen; therefore, a protective coating is necessary.<sup>37</sup> A new, two-step coating process has been developed to provide oxidation resistance for high-temperature (1,100–1,500°C) service.<sup>38</sup> First, a diffusion barrier of molybdenum or Mo-W alloy is applied to the niobium substrate using a conventional sputtering or chemical vapor deposition technique. Then the substrate is silicided to form a MoSi<sub>2</sub> or (Mo,W)Si<sub>2</sub> layer by a NaF-activated, pack-cementation method. Molybdenum disilicide has excellent high-temperature oxidation resistance, providing a thin protective SiO<sub>2</sub> oxygen barrier.

Because of the large mismatch in CTE between MoSi<sub>2</sub> and SiO<sub>2</sub>, the siliciding



treatment has been modified to codeposit silicon and germanium and thereby produce a  $\text{Mo}(\text{Si,Ge})_2$  or  $(\text{Mo,W})(\text{Si,Ge})_2$  diffusion layer. Because the stabilities for the volatile fluorides of silicon and germanium are reasonably similar, codeposition of silicon and about 3–8 at. % Ge to form  $(\text{Mo,W})(\text{Si,Ge})_2$  has been achieved using mixtures of pure silicon and germanium powders with a NaF activator at 1,150°C for 16 h. Small germania additions to silica greatly increase its CTE, and thereby decrease the CTE mismatch between the scale and the substrate, which improves the cyclic oxidation behavior of the coating.<sup>39</sup>

In a recent study, six out of eight  $(\text{Mo,W})(\text{Si,Ge})_2$ -coated pure niobium coupons survived cyclic oxidation in air for 200 one-hour periods at 1,370°C with weight-gains of only 1.2–1.6 mg/cm<sup>2</sup>. Premature failures occurred on two coupons due to excessive growth of  $\text{Nb}_2\text{O}_5$  initiated at cracks in the coating, but the  $\text{Nb}_2\text{O}_5$  formation was not catastrophic. One of the cyclic oxidation tests of a  $(\text{Mo,W})(\text{Si,Ge})_2$ -coated coupons was extended to 500 h cycles without failure.<sup>38</sup> These results indicate that this multi-component silicide coating offers significant promise to protect niobium-base alloys in oxidizing environments at very high temperatures.

## ACKNOWLEDGEMENTS

The research reported here has been sponsored by Oak Ridge National Laboratory (R.R. Judkins, contract FWP-FEAA028) and by the Naval Air Development Center/Office of Naval Research (M. Thomas, T. Kircher, J. Sedriks, grant N00014-90-J-1765). The authors acknowledge the preliminary support by the Electric Power Research Institute (J. Stringer). Important contributions to this research have been made by E.L. Courtright (Pacific Northwest Labs), J.L. Smialek and N. Jacobson (NASA-Lewis), and by A.J. Mueller, E.R. Naylor, F.D. Geib, and S.C. Kung during their studies at Ohio State University.

## References

1. C. Wagner, *Corr. Sci.*, 5 (1965), p. 751.
2. G. Allison and M.K. Hawkins, *GEC Rev.*, 17 (1914), p. 947.
3. M.G. Hocking, V. Vasantasree, and P.S. Sidky, *Metal & Ceramic Coatings: Production, High Temperature Properties and Applications* (New York: John Wiley & Sons, 1989), p. 174.
4. R.A. Rapp, D. Wang, and T. Weisert, "Simultaneous Chromizing-Aluminizing of Iron and Iron-Base Alloys by Pack Cementation," *High Temperature Coatings*, ed. M. Khobaib and R.C. Krutenat (Warrendale, PA: TMS, 1987), p. 131.
5. D.M. Miller et al., *Oxid. Met.*, 29 (1988), p. 239.
6. M.A. Harper and R.A. Rapp, "Codeposition of Chromium and Silicon in Diffusion Coatings for Iron-Base Alloys Using Pack Cementation," *Surface Modification Technologies IV*, ed. T.S. Sudarshan, D.G. Bhat, and M. Jeandin (Warrendale, PA: TMS, 1991), p. 415.
7. R. Bianco and R.A. Rapp, "Simultaneous Chromizing and Aluminizing of Nickel-Base Superalloys with Reactive Element Additions," *High Temperature Materials Chemistry V*, ed. W.B. Johnson and R.A. Rapp (Pennington, NJ: Electrochem. Soc., 1990), p. 211.
8. N.V. Bangaru and R.C. Krutenat, *J. Vac. Sci. Tech.*, B2 (1984), p. 806.
9. H.W. Grünling and R. Bauer, *Thin Solid Films*, 95 (1982), p. 1.
10. S.R. Levine and R.M. Caves, *J. Electrochem. Soc.*, 121 (1974), p. 1051.
11. B.K. Gupta, A.K. Sarkhel, and L.L. Seigle, *Thin Solid Films*, 39 (1976), p. 313.
12. B.K. Gupta and L.L. Seigle, *Thin Solid Films*, 73 (1980), p. 365.
13. F.J. Pennisi, N. Kandasamy, and L.L. Seigle, *Thin Solid Films*, 84 (1981), p. 17.
14. L.L. Seigle, *Surface Engineering*, ed. R. Kossowsky and S.C. Singhal (Boston, MA: Martinus Nijhoff Publishers, 1984), p. 345.
15. B. Nciri and L. Vandenbulke, *J. Less-Common Met.*, 95 (1983), p. 55.
16. S.C. Kung and R.A. Rapp, *J. Electrochem. Soc.*, 135 (1988), p. 731.
17. S.C. Kung and R.A. Rapp, *Oxid. Met.*, 32 (1989), p. 89.
18. V.A. Ravi, P. Choquet, and R.A. Rapp, "Thermodynamics of Simultaneous Chromizing-Aluminizing in Halide-Activated Cementation Packs," *International Meeting on Advanced Materials*, vol. 4 (Pittsburgh, PA: MRS, 1989), p. 483.
19. J.E. Restall, U.S. patent 4,687,684 (1987).
20. P.N. Walsh, *Proceeding of the Fourth International Conference on Chemical Vapor Deposition*, ed. G.F. Wakefield and J.M. Blocher (Pennington, NJ: Electrochem. Soc., 1973), p. 147.
21. W. Johnson, K. Komarek, and E. Miller, *Trans. AIME*, 242 (1968), p. 1685.
22. G.H. Marijnissen, *First International Conference on Surface Engineering*, vol. III (Brighton, U.K.: 1985), p. 81.
23. H. Flynn, A.E. Morris, and D. Carter, "An Iterative Gas-Phase Removal Version of SOLGASMIX," *Proceedings of the 25th CIM Conference of Metallurgists* (Toronto, Canada: TMS-CIM, 1986).
24. R. Bianco, R.A. Rapp, and N.S. Jacobson, submitted to *Oxidation of Metals*.
25. R.L. McCarron, N.R. Lindblad, and D. Chatterji, *Corrosion*, 32 (1976), p. 476.
26. C.A. Barrett, *Oxid. Met.*, 30 (1988), p. 361.
27. J. Jedlinski and S. Mrowec, *Mater. Sci. Eng.*, 87 (1987), p. 281.
28. G.W. Goward and D.H. Boone, *Oxid. Met.*, 3 (1971), 475.
29. J.H. DeVan, "Oxidation Behavior of Fe<sub>3</sub>Al and Derivative Alloys," *Oxidation of High Temperature Intermetallics*, ed. T. Grobstein and J. Doychak (Warrendale, PA: TMS, 1989), p. 107.
30. F.D. Geib and R.A. Rapp, "Diffusion Coatings for Iron Aluminide Fe<sub>3</sub>Al via Halide-Activated Pack Cementation," *Processing and Manufacturing of Advanced Materials for High Temperature Applications*, ed. T.S. Srivatsan and V.A. Ravi (Warrendale, PA: TMS, in press).
31. C.T. Liu, E.H. Lee, and C.G. McKamey, *Scripta Met.*, 23 (1990), p. 875.
32. J.L. Smialek, J. Doychak, and D.J. Gaydos, *Oxid. Met.*, 34 (1990), p. 259.
33. M.A. Harper and R.A. Rapp, "Chromized/Siliconized Diffusion Coatings for Iron-Base Alloys by Pack Cementation" (Paper number 66, presented at Corrosion 91, Cincinnati, OH, March, 1991).
34. W. Christl, A. Rahmel, and M. Schutze, *Oxid. Met.*, 31 (1989), p. 1.
35. K. Natesan and J.H. Park, "Role of Alloying Additions in the Oxidation-Sulfidation of Fe-Base Alloys," *Corrosion & Particle Erosion at High Temperatures*, ed. V. Srinivasan and K. Vedula (Warrendale, PA: TMS, 1989), p. 49.
36. M.A. Harper and R.A. Rapp, "Chromized/Siliconized Pack Cementation Diffusion Coatings for Heat Resistant Alloys," *First International Conference on Heat-Resistant Materials* (Materials Park, OH: ASM, to be published).
37. R.A. Perkins and G.H. Meier, *JOM*, 42 (1990), p. 17.
38. A.J. Mueller et al., submitted to *J. Electrochem. Soc.*
39. J. Schlichting and S. Neumann, *J. Non-Crystal. Solids*, 48 (1982), p. 185.

## ABOUT THE AUTHORS

**Robert Bianco** earned his M.Sc. in metallurgical engineering at the Ohio State University in 1991. He is currently a Ph.D. candidate at Ohio State. Mr. Bianco is also a member of TMS.

**Mark A. Harper** earned his M.Sc. in materials science and engineering at the Ohio State University in 1991. He is currently a Ph.D. candidate at Ohio State. Mr. Harper is also a member of TMS.

**Robert A. Rapp** earned his Ph.D. in metallurgical engineering at Carnegie Mellon University in 1959. He is currently a professor at Ohio State. Dr. Rapp is also a member of TMS.

If you want more information on this subject, please circle reader service card number 50.

